



Global Biogeochemical Cycles

RESEARCH ARTICLE

10.1029/2020GB006612

Special Section:

Fire in the Earth System

Key Points:

- Potential evapotranspiration was a significant driver of carbon stocks and their post-fire recovery
- Carbon stocks accumulated at a rate of $2\text{--}60 \text{ g m}^{-2} \text{ yr}^{-1}$ during the first 100 years after forest fire
- If the fire return interval shortens to ≤ 100 years, many boreal forests will be prevented from reaching their full carbon storage potential

Correspondence to:

M. Palviainen,
marjo.palviainen@helsinki.fi

Citation:

Palviainen, M., Laurén, A., Pumpanen, J., Bergeron, Y., Bond-Lamberty, B., Larjavaara, M., et al. (2020). Decadal-scale recovery of carbon stocks after wildfires throughout the boreal forests. *Global Biogeochemical Cycles*, 34, e2020GB006612. <https://doi.org/10.1029/2020GB006612>

Received 25 MAR 2020

Accepted 29 JUL 2020

Accepted article online 11 AUG 2020

Decadal-Scale Recovery of Carbon Stocks After Wildfires Throughout the Boreal Forests

M. Palviainen¹ , A. Laurén², J. Pumpanen³ , Y. Bergeron⁴ , B. Bond-Lamberty⁵ , M. Larjavaara⁶ , D. M. Kashian⁷ , K. Köster¹, A. Prokushkin⁸, H. Y. H. Chen^{9,10}, M. Seedre¹¹ , D. A. Wardle¹², M. J. Gundale¹³, M.-C. Nilsson¹³, C. Wang^{14,15}, and F. Berninger¹⁶

¹Department of Forest Sciences, University of Helsinki, Helsinki, Finland, ²Faculty of Science and Forestry, University of Eastern Finland, Joensuu, Finland, ³Department of Environmental and Biological Sciences, University of Eastern Finland, Kuopio, Finland, ⁴Forest Research Institute, Université du Québec en Abitibi-Témiscamingue and Centre for Forest Research, Université du Québec à Montréal, Montreal, Canada, ⁵Joint Global Change Research Institute, Pacific Northwest National Laboratory, College Park, MD, USA, ⁶Institute of Ecology and Key Laboratory for Earth Surface Processes of the Ministry of Education, College of Urban and Environmental Sciences, Peking University, Beijing, China, ⁷Department of Biological Sciences, Wayne State University, Detroit, MI, USA, ⁸V.N. Sukachev Institute of Forest SB RAS, Krasnoyarsk, Russia, ⁹Faculty of Natural Resources Management, Lakehead University, Thunder Bay, Canada, ¹⁰Key Laboratory for Humid Subtropical Eco-Geographical Processes of the Ministry of Education, Fujian Normal University, Fuzhou, China, ¹¹Southern Swedish Forest Research Centre, Swedish University of Agricultural Sciences, Uppsala, Sweden, ¹²Asian School of the Environment, Nanyang Technological University, Singapore, ¹³Department of Forest Ecology and Management, Swedish University of Agricultural Sciences, Umeå, Sweden, ¹⁴Center for Ecological Research, Northeast Forestry University, Harbin, China, ¹⁵Key Laboratory of Sustainable Forest Ecosystem Management-Ministry of Education, Northeast Forestry University, Harbin, China, ¹⁶Department of Environmental and Biological Sciences, University of Eastern Finland, Joensuu, Finland

Abstract Boreal forests store 30% of the world's terrestrial carbon (C). Consequently, climate change mediated alterations in the boreal forest fire regime can have a significant impact on the global C budget. Here we synthesize the effects of forest fires on the stocks and recovery rates of C in boreal forests using 368 plots from 16 long-term (≥ 100 year) fire chronosequences distributed throughout the boreal zone. Forest fires led to a decrease in total C stocks (excluding mineral soil) by an average of 60% (range from <10% to >80%), which was primarily a result of C stock declines in the living trees and soil organic layer. Total C stocks increased with time since fire largely following a sigmoidal shape Gompertz function, with an average asymptote of 8.1 kg C m^{-2} . Total C stocks accumulated at a rate of $2\text{--}60 \text{ g m}^{-2} \text{ yr}^{-1}$ during the first 100 years. Potential evapotranspiration (PET) was identified as a significant driver of C stocks and their post-fire recovery, likely because it integrates temperature, radiation, and the length of the growing season. If the fire return interval shortens to ≤ 100 years in the future, our findings indicate that many boreal forests will be prevented from reaching their full C storage potential. However, our results also suggest that climate warming-induced increases in PET may speed up the post-fire recovery of C stocks.

1. Introduction

Wildfires significantly affect the global C cycle and climate (Li et al., 2017; Pellegrini et al., 2018; Walker et al., 2019). Global CO₂ emissions from fires are estimated to be 2.2 Pg C annually (van der Werf et al., 2017), which corresponds to 20% of those from fossil fuel combustion (Le Quéré et al., 2018). Climate change is projected to increase the risk of wildfires (de Groot, Flannigan, et al., 2013; Flannigan et al., 2009), and the extent, frequency, and intensity of forest fires have already increased during recent decades in the circumboreal region (Kasischke & Turetsky, 2006; Ponomarev et al., 2016; Williams et al., 2016). As boreal forests store more than 30% of the world's terrestrial C (Pan et al., 2011), changes in their fire regimes may have significant implications for the global C balance (Pellegrini et al., 2018). Although fire management and suppression operations have reduced the occurrence of fires in many inhabited parts of boreal forests, notably in Fennoscandia (Wallenius, 2011), wildfires are a dominant driver of ecosystem dynamics and weaken the C sink strength of boreal forests (Bond-Lamberty et al., 2007; Walker et al., 2019). Currently, 10–15 million hectares of boreal forest burn annually (Flannigan et al., 2009), and this is estimated to double in the future (Flannigan et al., 2009; Lehtonen et al., 2016; Ponomarev et al., 2016).

Quantifying the post-fire C changes and the recovery rate of C stocks is necessary for understanding how changing fire activity can influence regional and global C budgets in both short and long time scales (Pellegrini et al., 2018; Walker et al., 2019). Fires reduce forest C stocks in the short term (Kashian et al., 2013; Köster et al., 2016; Seedre et al., 2014; Wang et al., 2003) and increase CO₂ emissions to the atmosphere (Ghimire et al., 2012; van der Werf et al., 2017). Over longer time scales, fires can affect C dynamics by altering forest regrowth (Johnstone et al., 2016; Kashian et al., 2013), succession (Williams et al., 2016), organic matter decomposition (Aaltonen et al., 2019; Dooley & Treseder, 2012; O'Neill et al., 2006), permafrost thawing (Köster et al., 2017), and the fluxes of energy and nutrients (Palviainen et al., 2017; Randerson et al., 2006; Wirth et al., 2002).

Fires can greatly affect the C stocks of living and dead biomass, as well as soil C stocks (Kashian et al., 2013; Köster et al., 2016; Seedre et al., 2014). Crown fires cause tree mortality and transfer C from live to dead pools (Kashian et al., 2013; Köster et al., 2016; Seedre et al., 2014). During the early post-fire stage, C accumulation in regenerating vegetation is often less than C released through decomposition (Amiro et al., 2010). The turning point at which the post-fire boreal stands switch from a C source to sink is still unclear. Following the fire event, biomass typically accumulates over time until it stabilizes (Bormann & Likens, 1979; Ward et al., 2014) or starts to decrease (Wardle et al., 2004). As a consequence of surface fires, the C stock in the soil organic layer (O-layer) is frequently reduced through combustion and reduced litter inputs and starts to increase after the recovery of vegetation (Andrieux et al., 2018; Czimczik et al., 2005; Nave et al., 2011). Over time, C stocks in the O-layer level off (Taylor et al., 2014; Ward et al., 2014), decline (Gao et al., 2018), or continue to increase, both in paludified sites (Simard et al., 2007) and when the sites become dominated by late-successional plant species that produce recalcitrant litter (Wardle et al., 2003). In contrast, the mineral soil C stock usually remains relatively unchanged following fire (DeLuca & Boisvenue, 2012; Harden et al., 1992; Seedre et al., 2011). Quantifying the time needed for post-fire ecosystems to recover to their previous state is essential because if the fire intervals become shorter than the recovery time, C stocks would not reach their pre-fire C storage capacity (Bartowitz et al., 2019; Johnstone et al., 2016; Turner et al., 2019), potentially altering the role of boreal forests in the global C cycle.

Fire severity affects tree mortality, organic matter combustion, as well as the recruitment and growth of regenerating vegetation, and thus the rate of C accumulation (Ghimire et al., 2012; Johnstone et al., 2016; van Bellen et al., 2010; Williams et al., 2016). Severe, stand-replacing crown fires are dominant in North American boreal forests, whereas lower-intensity surface fires are common in Eurasian boreal forests (de Groot, Cantin, et al., 2013). High-severity crown fires kill most trees and combust large amounts of detritus, although they do not wholly consume the trees they kill (Stenzel et al., 2019). Ground fires, in turn, typically do not kill healthy mature trees and may combust less organic matter. The dominant tree species in North American boreal forests (such as *Picea mariana* and *Pinus banksiana*) have highly flammable needles and low, dense live branches, which promote the incidence of crown fires (Rogers et al., 2015). The dominant tree species in Eurasian boreal forests often have thick bark (e.g., *Pinus sylvestris*), a capacity for self-pruning, and in the case of larch (*Larix gmelinii*), high leaf moisture content, which increases their fire resistance and chances of surviving fire.

In old-growth forests, total ecosystem C has been shown to either decrease (Gao et al., 2018) or slowly continue to accumulate (Law et al., 2003; Luyssaert et al., 2008; Wardle et al., 2003) over time, especially in dead organic matter pools (Kurz et al., 2013; Zhou et al., 2006). The divergent C accumulation patterns observed among studies indicate a knowledge gap in the processes that regulate C dynamics in boreal forests following fire. It is plausible that divergent patterns of C accumulation among chronosequences could reflect differences in fire severity, forest site productivity, climatic conditions, or initial C stocks, but this remains unclear.

The primary objective of this study is to synthesize the effects of wildfires on the C stocks and their recovery rates in boreal forests. We compiled data from published and unpublished fire chronosequence studies throughout the boreal zone and addressed the following questions:

1. To what extent do wildfires decrease C stocks in boreal forests?
2. How do fires change C distribution among different ecosystem components?
3. How quickly do forest C stocks recover after fire, and how does the recovery rate vary across the boreal zone?



Figure 1. Geographical location of studied forest fire chronosequences.

4. To what extent do time since fire, climatic conditions, and fire severity explain the variation in the C accumulation rate?

Answering these questions, and thus understanding the recovery patterns and driving mechanisms of post-fire C dynamics, is a prerequisite for assessing the capacity of boreal forests to sequester and store C and for predicting the response of boreal ecosystem functions and resilience to climate change and altered fire regime.

2. Materials and Methods

2.1. Chronosequences

We compiled data from boreal and oroboreal forests (Figure 1). The data included a total of 368 plots from 16 fire chronosequence studies (Table 1). The chronosequence, or space for time approach, is a commonly used and effective method to study long-term recovery processes following disturbance (Walker et al., 2010). The mean annual temperature in the study areas ranged from -9.5°C to $+5.2^{\circ}\text{C}$, and the mean annual precipitation ranged from 295 to 824 mm. Chronosequences were located between the latitudes 44°N and 67°N and covered the dominant vegetation groupings in North American, North European, and Russian boreal forests. Soils were Haplic Podzols (chronosequences 1, 2, 3, 9, 13, 14, and 15; numbering corresponds to Table 1), Cryosols (4), Brunisols (5), Gray Luvisols or Luvic Gleysols (6, 7, 8), Typic Hapl cryalfs (10), Typic Hapl turbels, Typic Eutro cryepts, Typic Haplorthels, and Typic Aquorthels (11, 12, 16). The chronosequences 4, 11, 12, and 16 (see Table 1) belong to the continuous permafrost zone, whereas the others are in discontinuous or permafrost-free zones. Detailed descriptions of these chronosequences can be found in the literature (Bond-Lamberty et al., 2002; DeLuca et al., 2002; Kashian et al., 2013, Köster et al., 2014, 2016, 2017, 2018; Larjavaara et al., 2017; Lecomte et al., 2006; Seedre et al., 2014; Wang et al., 2003; Wirth et al., 2002).

Across the 16 chronosequences, the size of the sample plots varied from 50 to $5,000\text{ m}^2$ (Table 2). The C stocks in living trees, ground vegetation, lying dead trees, standing dead trees (snags), and the O-layer were measured. Data from Yukon, Canada (chronosequences 4 and 5), and from Tura, Siberia (chronosequences 11 and 12), were collected for this study, and the rest of the data have been published previously (Tables 1 and 2). Above-ground tree biomass was calculated using tree measurements (height, breast height diameter, crown length, and crown diameter) and species-specific allometric equations (Kashian et al., 2013; Lambert et al., 2005; Larjavaara et al., 2017; Marklund, 1988; Paré et al., 2013; Repola, 2008; 2009; Wang et al., 2003). The necromass of dead trees was estimated similarly to that of living tree biomass, except that decay class-specific deadwood density values were used in calculating biomass from measured volumes. Ground vegetation was clipped from $0.07\text{--}1\text{ m}^2$ quadrats (Table 2), oven dried to a constant mass, and weighed. From one to ten volumetric samples of the O-layer down to the mineral soil were collected from each plot (Table 2). The C stocks of living and dead vegetation were determined by multiplying their biomass either with measured C concentrations or assuming 45–50% C content. The C stocks of the soil O-layer were calculated by multiplying the C concentration of samples with their bulk densities and layer depths. Concentrations of C were measured using elemental analyzers (varioMAX CN elemental analyzer,

Table 1

Location, Time Since Fire, Mean Annual Temperature (MAT), Mean Temperature in January and July, Mean Annual Precipitation (MAP), Dominant Tree Species, and Soil Texture in the Study Sites

Chronosequence	Site	Coordinates	Time since fire (years)	MAT (°C)	January temperature (°C)	July temperature (°C)	MAP (mm)	Dominant tree species	Soil texture
1	Finland, Lapland	67°46' N, 29°35' E	2–156	-0.9	-12.7	14.0	592	<i>Pinus sylvestris</i>	Loamy sand
2	Sweden, Arvidsjaur	65°35'– 66°07' N, 17°15'– 19°26' E	49–322	-2.0	-13.5	13.7	600	<i>Pinus sylvestris, Betula pubescens, Picea abies</i>	Sand
3	Estonia, Vihterpalu	59°10'– 59°14' N, 23°36'– 23°49' E	7–178	+5.2	-4.9	17.1	642	<i>Pinus sylvestris</i>	Loamy sand
4	Canada, Yukon North	66°22'– 67°26' N, 133°45'– 136°43' W	3–115	-8.8	-29.5	10.8	248	<i>Picea mariana, Picea glauca</i>	Silty clay loam
5	Canada, Yukon South	62°40' N, 136°11' E	2–115	-3.4	-24.4	11.1	295	<i>Picea mariana</i>	Silty clay loam
6	Canada, Manitoba D (dry site)	55°53' N, 98°20' W	3–151	+0.8	-24.1	16.6	439	<i>Picea mariana, Pinus banksiana, Populus tremuloides</i>	Silty clay loam
7	Canada, Manitoba W (wet site)	55°53' N, 98°20' W	3–151	+0.8	-24.1	16.6	439	<i>Picea mariana, Pinus banksiana, Populus tremuloides</i>	Silty clay loam
8	Canada, Quebec	49°57' N, 79°10' W	11–356	+0.9	-18.4	16.6	824	<i>Picea mariana</i>	Clay
9	Canada, Ontario	49°40'– 49°65' N, 89°21'– 89°68' W	1–203	-1.2	-18.2	16.6	725	<i>Pinus banksiana, Picea mariana, Populus tremuloides, Abies balsamea</i>	Silty/loamy sand
10	USA, Yellowstone	44°45' N, 110°67' W	24–328	+3.9	-7.7	17.5	620	<i>Pinus contorta</i>	Sandy loam
11	Russia, Tura South 1	64°37' N, 100°28' E	1–154	-9.5	-35.9	16.6	380	<i>Larix gmelinii</i>	Silt loam
12	Russia, Tura South 2	64°37' N, 100°28' E	1–100	-9.5	-35.9	16.6	380	<i>Larix gmelinii</i>	Silt loam
13	Russia, Yenisei river 1	60°43' N, 89°08' E	12–266	-3.7	-17.0	16.5	493	<i>Pinus sylvestris</i>	Sand
14	Russia, Yenisei river 2	60°43' N, 89°08' E	67–383	-3.7	-17.0	16.5	493	<i>Pinus sylvestris</i>	Sand
15	Russia, Yenisei river 3	60°43' N, 89°08' E	14–244	-3.7	-17.0	16.5	493	<i>Pinus sylvestris</i>	Sand
16	Russia, Irkutsk, Oblast	60°75' N, 107°75' E	44–218	0	-31.3	16.7	401	<i>Larix gmelinii</i>	Silt loam

Note. References for chronosequences: 1 = Köster et al. (2014), 2 = DeLuca et al. (2002), 3 = Köster et al. (2016), 4 = Pumpanen et al. (unpublished data), 5 = Pumpanen et al. (unpublished data), 6 = Bond-Lamberty et al. (2002), Wang et al. (2003), 7 = Bond-Lamberty et al. (2002), Wang et al. (2003), 8 = Lecomte et al. (2006), 9 = Seedre et al. (2014), 10 = Kashian et al. (2013), 11 = Prokushkin et al. (unpublished data), 12 = Pumpanen et al. (unpublished data), 13 = Wirth et al. (2002), 14 = Wirth et al. (2002), 15 = Wirth et al. (2002), 16 = Larjavaara et al. (2017).

Elementar Analysensysteme GmbH, Germany or LECO CNS 2000 analyzer, LECO Corporation, St Joseph, MI, USA).

2.2. Data Analysis

The study focuses on sites where time since fire is ≤ 200 years because data were scarce for the older sites. Raw data are presented in Figure 2. Data in each chronosequence were classified into 20-year intervals,

Table 2

The Number of Study Plots Per Age Class (Time Since Fire), Size of the Study Plots, the Number of Ground Vegetation Quadrats Per Plot, the Size of the Ground Vegetation Biomass Quadrats, and the Number of Soil Samples

Chronosequence	Site	No. of study plots per age class	Size of the study plots (m^2)	No. of ground vegetation quadrats per plot	Size of ground vegetation quadrats per plot (m)	No. of soil samples per plot
1	Finland, Lapland	3	400	5	0.2×0.2	10
2	Sweden, Arvidsjaur	1–2	314	10	0.5×0.5	10
3	Estonia, Vihterpalu	3	400	2	0.2×0.2	5
4	Canada, Yukon North	9	400	4	0.2×0.2	1
5	Canada, Yukon South	9	400	4	0.2×0.2	1
6	Canada, Manitoba D (dry site)	4–5	50	6	0.25×0.25	5
7	Canada, Manitoba W (wet site)	4–5	50	6	0.25×0.25	5
8	Canada, Quebec	1–4	400	4	0.25×0.25	5
9	Canada, Ontario	3	400	5	1.0×1.0	10
10	USA, Yellowstone	4–6	500	n.d.	n.d.	5
11	Russia, Tura South 1	1	100–800	10	0.25×0.25	6
12	Russia, Tura South 2	9	400	4	0.2×0.2	1
13	Russia, Yenisei river 1	1	100–750	n.d.	n.d.	3–5
14	Russia, Yenisei river 2	1	225–5,000	n.d.	n.d.	3–5
15	Russia, Yenisei river 3	1	200–5,000	n.d.	n.d.	3–5
16	Russia, Irkutsk, Oblast	1–13	314	2	0.07×0.07	2

Note. References for chronosequences: 1 = Köster et al. (2014), 2 = DeLuca et al. (2002), 3 = Köster et al. (2016), 4 = Pumpanen et al. (unpublished data), 5 = Pumpanen et al. (unpublished data), 6 = Bond-Lamberty et al. (2002), Wang et al. (2003), 7 = Bond-Lamberty et al. (2002), Wang et al. (2003), 8 = Lecomte et al. (2006), 9 = Seedre et al. (2014), 10 = Kashian et al. (2013), 11 = Prokushkin et al. (unpublished data), 12 = Pumpanen et al. (unpublished data), 13 = Wirth et al. (2002), 14 = Wirth et al. (2002), 15 = Wirth et al. (2002), 16 = Larjavaara et al. (2017).

Abbreviation: n.d., not determined.

and the mean C stock within the interval was computed. C stocks at selected time points were then calculated by linear interpolation between the consecutive mean values (Figure 2). We did not extrapolate outside the extent of the chronosequence. Stocks of C and the proportion of living trees, ground vegetation, O-layer, and dead trees of the total C stock were assessed for the selected time points (Figure 3). To characterize fire severity, we recalculated ecosystem C stocks as C stock divided by the chronosequence maximum total C stock, resulting in a 0–1 scalar that varied as a function of time since fire (Figure 5).

To describe C stocks in different ecosystem components as a function of time since fire, we fitted widely used continuous nonlinear model types, such as Gompertz, Chapman-Richards, Michaelis-Menten, and polynomial functions, to the measured data (see e.g., Kashian et al., 2013). Nonlinear mixed effect models were used to study the variation of C stocks and to explain it by using time since fire and key climatic variables. The following variables were used in the analyses: mean annual temperature, mean annual precipitation (mm), potential evapotranspiration (PET), mean summer (June–August) temperature, mean summer (June–August) precipitation, and Palmer's drought severity index (PDSI; Palmer, 1965). The long-term climatic data and PDSI for the study sites were derived from the Climatic Research Unit (CRU) database (New et al., 2000), which provides medium-resolution (0.5° latitude \times 0.5° longitude grid) global monthly climate data. First, we compiled a basic model containing time since fire, and we then tested whether the model's predictive ability could be improved by adding the above-mentioned climatic variables (Table 3).

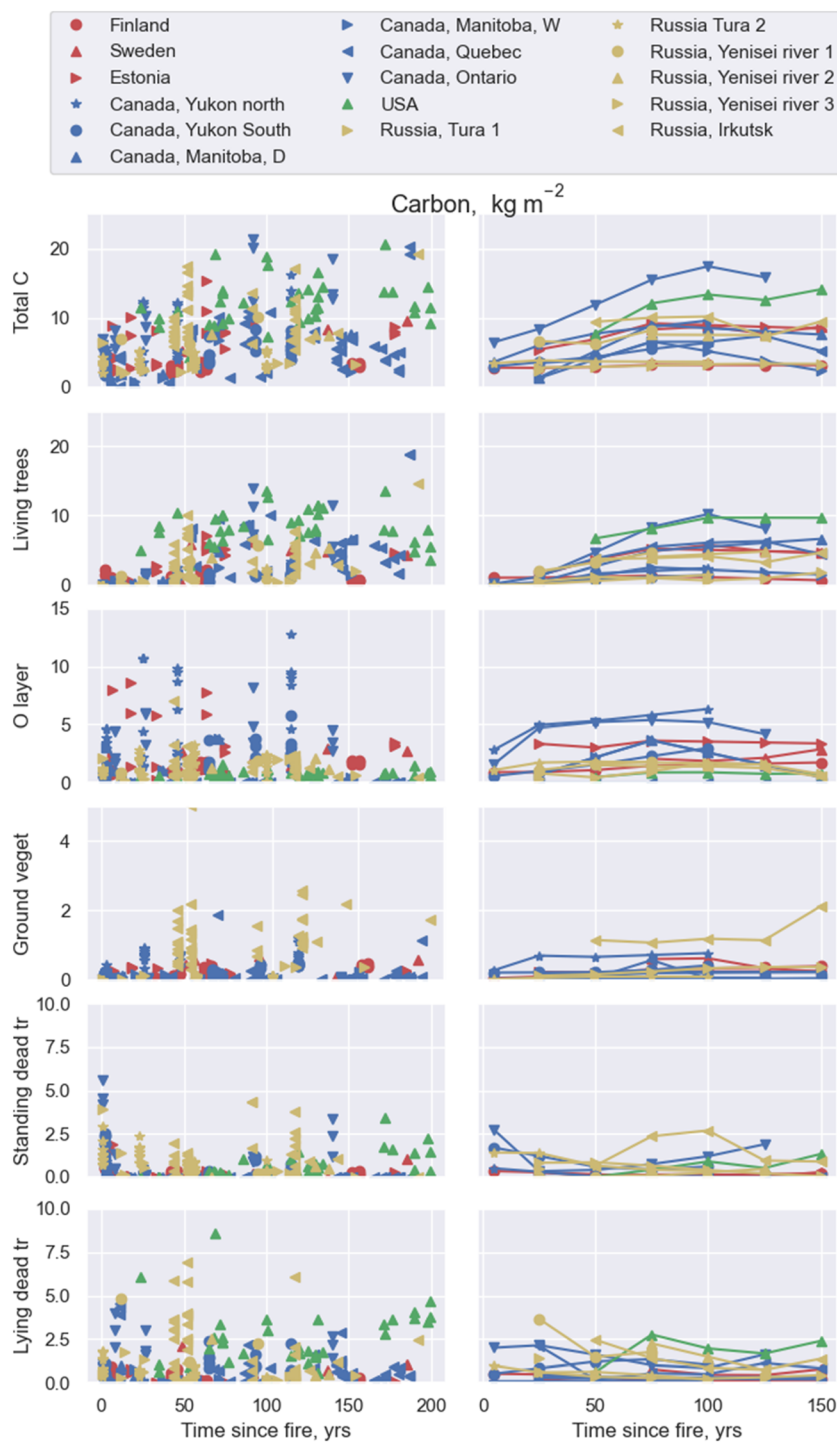


Figure 2. Carbon stocks (kg m^{-2}) in ecosystem, living trees, organic layer, ground vegetation, standing dead trees, and lying dead trees in the studied boreal forest fire chronosequences. Raw data are presented on the left panel, and the linearly interpolated data for 20-year intervals are presented on the right panel.

Models were fit to the raw (measured) data using the nlme package in R version 3.4.3. The best models were selected based on Akaike information criteria (AIC) values.

Our primary interest was the total C stock in the forest, which is composed of different components (living trees, ground vegetation, dead trees, and O-layer). Environmental factors are likely to affect these

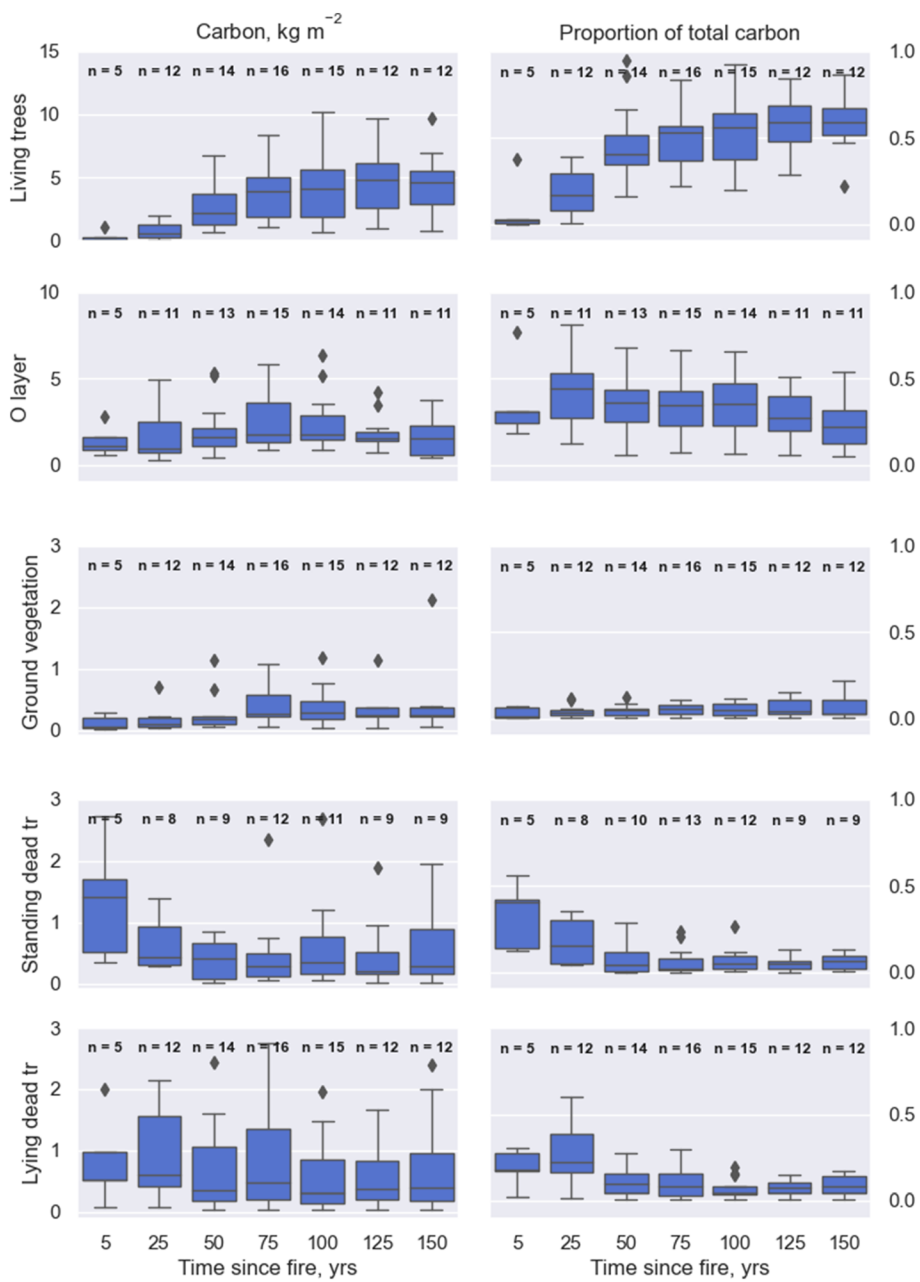


Figure 3. Carbon stocks (C kg m^{-2}) in living trees, ground vegetation, organic layer, standing dead trees, and lying dead trees and their proportion of the total C stock. The boxes represent the interquartile range (50% of values), whiskers represent 95% of values, and horizontal lines in the boxes represent median. The boxplots represent measured and linearly interpolated values (see section 2), and n above the boxplots indicates the number of replicates.

components and thus total C. To examine these factors, we used structural equation modeling (SEM), a form of path analysis that is used to study causal dependencies and relationships between variables and to identify the relative importance of different potentially influential factors (Fan et al., 2016). The starting point of the SEM analysis was a preliminary causal network, where total C stock depends on the living and dead trees, ground vegetation, and soil C stocks and on the environmental factors affecting these variables. We used SEM to evaluate the factors regulating post-fire C stocks of different ecosystem components and possible correlations among the influencing factors (Figure 6). The analysis proceeds as an iterative loop from the model parameter estimation to the interpretation of the parameter estimates and evaluation of their

significance and to the comparison of the goodness-of-fit (Fischer's C statistics and AIC) values between the different model structures. The procedure continues with a revised model structure until a better structure could not be found. We applied the SEM for time points 50, 75, and 100 years after fire because most of the C accumulation took place in this time range (Figure 5). Stands that were burned less than 50 years ago did not contain enough data for the SEM analyses. The same variables that were used as in the mixed effect models were also used as explanatory variables. Time since fire was not directly included in the SEM analyses because each C component has a different shape of time dependency, which would have made the interpretation of the time parameter cumbersome. The analyses were conducted on interpolated values in these time points (Figure 3) by using the piecewise SEM (Lefcheck, 2016) statistical R package (version 3.4.3, <http://www.r-project.org/>).

3. Results

Stocks of C in living trees varied from 0 to 2 kg m⁻² in recently burned stands and increased with time since fire up to 19 kg m⁻² over 180 years (Figure 2). These C stocks increased with time since fire following a sigmoidal shape Gompertz function (Table 3), which reached an average of 4.2 kg m⁻² 125 years after fire (Figure 3). We found that PET was the most important climatic variable describing the variation in C stocks in living trees (Table 3).

Carbon stocks of the O-layer were on average 50% lower in stands that had burned ≤25 years ago (1 kg m⁻²) than in mature stands that had been burned ≥75 years ago (Figure 3). On average, C stocks in the O-layer recovered in about 100 years and remained rather constant thereafter (Figure 3). The asymptote for the O-layer was 2.17 kg m⁻² (Table 3). Carbon stocks in the O-layer could be best described using a Gompertz function that included time since fire and summertime temperature (Table 3). Accumulation rates of C in the O-layer ranged from 1 to 30 g m⁻² yr⁻¹ during the first 100 years post-fire.

Stocks of C in standing dead trees were highly variable ranging from 0.2 to 6 kg m⁻² in recently burned stands (Figure 2). The largest C stocks in standing dead trees were observed in stands within 5 years of burning (Figure 3). The C stocks of lying dead trees also showed large variation shortly after fire; the smallest values were 0.1 kg m⁻², and the largest values were 5 kg m⁻² (Figure 2). Similar to living trees, PET was the most important climatic factor that explained variation in C stocks in lying dead trees (Table 3).

Stocks of C in ground vegetation were small. In general, they were less than 0.5 kg m⁻² shortly after fire and increased to a maximum of 1–2 kg m⁻² during post-fire succession (Figures 2 and 3). PET best described variation in C stocks of the ground vegetation, and there was an inverse relationship between PET and ground vegetation C pools (Table 3).

Total ecosystem C stocks, calculated by summing all of the above-mentioned C stocks, were 2–9 kg m⁻² shortly after fire and increased to 3–21 kg m⁻² within 100 years after fire (Figure 2). Total C stocks increased with time since fire following a Gompertz function (Figure 4). The best climatic variable that described the variation in total ecosystem C stocks was PET. Total C accumulation rates gradually decreased with time since fire (Figure 4). Total C stocks increased almost linearly until year 50 and then started to level off to 8 kg m⁻² at about year 75. The asymptote was 8.13 kg m⁻² (Table 3). Total C accumulation rates among the chronosequences varied considerably and ranged from 2 to 60 g m⁻² yr⁻¹ during the first 100 years.

Time since fire significantly affected the C partitioning between different pools (Figure 3). Immediately after fire, dead trees composed the largest C stock, accounting for an average of 60% of total ecosystem C. The second most important C stock was the O-horizon, with an average proportion of 30% total C. The C stock of standing dead trees was highest during the first 5 years after fire, but from 5 to 25 years after fire, most of these trees were transferred to the lying dead tree stock. After 50 years onwards, living trees were the most important C stock; they accounted for an average of roughly 60% of the total ecosystem C in old (>100 years) forests.

Fire severity varied markedly among the studied chronosequences (Figure 5). In the most severe stand-replacing fires, the initial C stock was only ≤20% of the maximum C stock, whereas after low-severity fires, forest C stock decreased only slightly (Figure 5). On average, fire caused a 60% decrease in ecosystem C stock (Figure 5). Most of the subsequent C accumulation took place during the first

Table 3
Parameters, Random Effects (α), Residuals (ε), Akaike's Information Criteria (AIC), and Degrees of Freedom (DFs) of the Nonlinear Mixed Effects Models Fitted for C Stocks (kg m^{-2}) in Different Ecosystem Components

Model	a_0 (SE, p value)	a (SE, p value)	b (SE, p value)	c (SE, p value)	d (SE, p value)	α (SE)	ε	AIC	DF
<i>Living trees = $(a + \alpha)e^{-be^{-ct}} + \varepsilon$</i>	4.217 (0.639, <0.0001)	9.809 (7.261, 0.178)	0.076 (0.021, <0.001)			2.376	2.243	1690.9	350
<i>Living trees = $a_0 + (a + \alpha)*PETe^{-be^{-ct}} + \varepsilon$</i>	-1.387 (1.400, 0.323)	3.891 (0.922, <0.0001)	9.759 (7.329, 0.184)	0.077 (0.022, <0.001)		1.511	2.245	1681.5	349
<i>O layer = $(a + \alpha)e^{-be^{-ct}} + \varepsilon$</i>		2.170 (0.398, <0.0001)	0.732 (0.286, 0.011)	0.061 (0.024, 0.012)		1.485	1.559	1430.0	350
<i>O layer = $a_0 + (a + \alpha)*TSe^{-be^{-ct}} + \varepsilon$</i>	5.338 (2.065, 0.010)	-0.266 (0.165, 0.108)	2.024 (1.075, 0.061)	0.339 (0.185, 0.068)		1.283	1.568	1427.9	349
<i>Ground vegetation = $(a + \alpha) + (bt)^*$</i>		0.157 (0.109, 0.153)	0.006 (0.004, 0.080)	0.987 (0.006, <0.0001)	0.0007 (0.006, 0.239)	0.311 (0.0006, 0.239)	0.363	279.9	273
<i>Ground vegetation = $(a_0 + (a + \alpha + b * PETs)^* t)^* c^t + dt + \varepsilon$</i>	0.120 (0.049, 0.153)	0.050 (0.020, 0.013)	-0.015 (0.007, 0.031)	0.991 (0.001, <0.0001)	0.0006 (0.004, 0.128)	2.1 × 10 ⁻⁵ (0.0004, 0.128)	0.360	272.4	272
<i>Standing dead trees = $(a + \alpha)^* (t - b)^2 + c + \varepsilon$</i>		0.00002 (0.00001, <0.0001)	131.812 (<0.0001)	0.344 (0.139, 0.014)		0.014 (0.139, 0.014)	0.855	969.0	350
<i>Standing dead trees = $(a + \alpha)^* (t - b)^2 + c + d * Prec + \varepsilon$</i>	0.00002 (0.00001, <0.0001)	179.214 (<0.0001)	35.016 (-0.0036)	0.241 (0.248, 0.332)	5.6 × 10 ⁻⁵ (0.0004, 0.332)	0.802 (0.248, 0.332)	930.8	349	
<i>Lying dead trees = $((a + \alpha) + bi)^* e^t + dt + \varepsilon$</i>	1.161 (0.161, <0.0001)	-0.015 (0.001, 0.072)	(0.001, 0.004)	<0.0001 (0.001, <0.0001)	-0.008 (0.002, <0.001)	1.083 (0.002, <0.001)	0.434	1152.3	349
<i>Lying dead trees = $(a_0 + ((a + \alpha) + bi)^* t)^* c^t + dt + \varepsilon$</i>	1.149 (0.177, <0.0001)	0.003 (0.002, 0.160)	-0.0035 (0.003, 0.204)	1.002 (0.001, <0.0001)	-0.007 (0.004, 0.088)	0.506 (0.004, 0.088)	1.072	1142.6	348
<i>Total C = $(a + \alpha)e^{-be^{-ct}} + \varepsilon$</i>		8.132 (0.942, <0.0001)	0.886 (0.128, <0.0001)	0.027 (0.006, <0.0001)		3.490 (0.006, <0.0001)	2.980 (0.006, <0.0001)	1904.8	350
<i>Total C = $a_0 + (a + \alpha)*PETe^{-be^{-ct}} + \varepsilon$</i>	2.748 (2.747, 0.318)	3.738 (1.815, 0.040)	0.881 (0.129, <0.0001)	0.027 (0.006, <0.0001)		3.044 (0.006, <0.0001)	2.982 (0.006, <0.0001)	1903.1	349

Note. t = time since fire, PET = potential evapotranspiration, T_S = summertime (June–August) air temperature, PET_S = summertime (June–August) potential evapotranspiration, $Prec$ = annual precipitation.

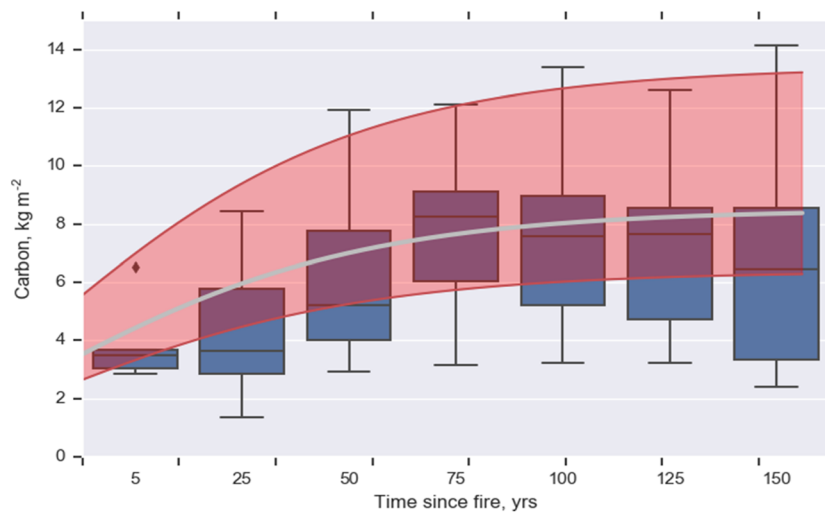


Figure 4. Total ecosystem carbon stock (C kg m^{-2}) and Gompertz function describing the accumulation of total C (see bottom row in Table 3). The boxes represent the interquartile range (50% of values), whiskers represent 95% of values, and horizontal lines in the boxes represent median. The red range describes the variation originating from the range in potential evapotranspiration (PET).

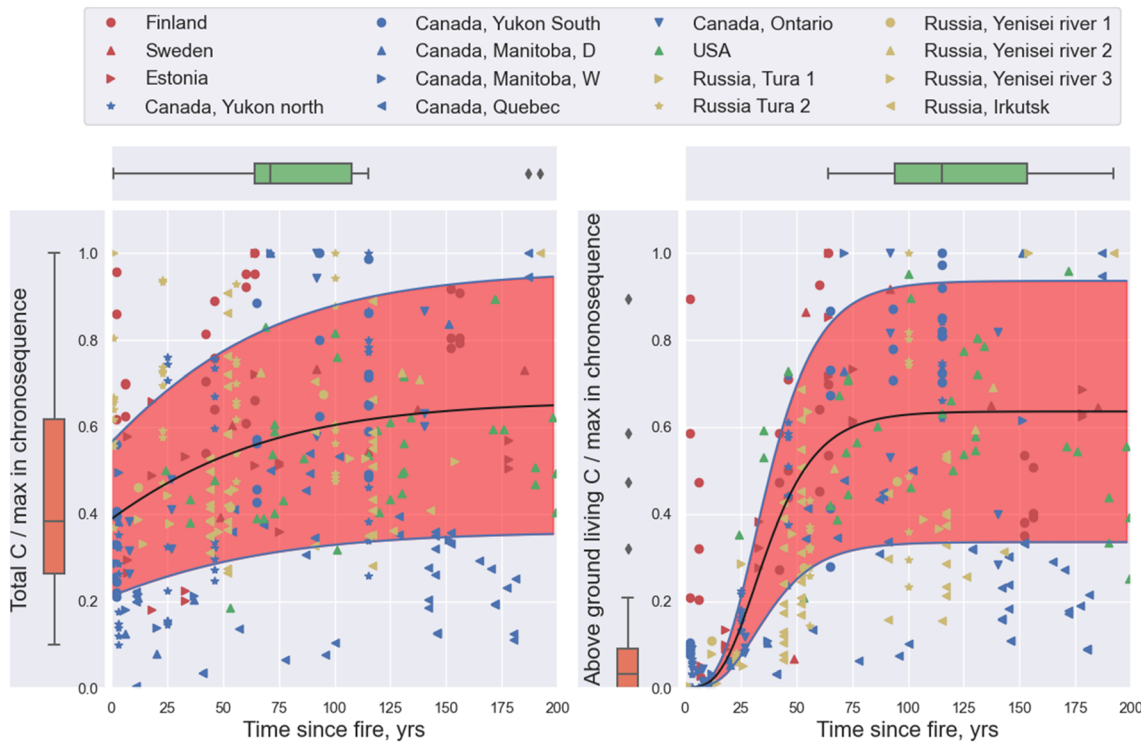


Figure 5. The proportion of total C stock of the chronosequence maximum total C stock as a function of time since fire (on the left) and the proportion of living above-ground biomass C stock of the chronosequence maximum living above-ground biomass C stock as a function of time since fire (on the right). The black line represents the average value of all chronosequences, and the area highlighted with red is the 95% confidence interval. Note that different chronosequences reach their maximum C storage at different age, and therefore, the mean curve does not reach 1. A boxplot on the left-hand side of y axis describes the variation in fire severity. The boxplot includes data from ≤ 10 years after fire. Horizontal boxplot indicates the distribution of time required to reach the maximum C stock. The boxes represent the interquartile range (50% of values), whiskers represent 95% of values, and horizontal lines in the boxes represent median.

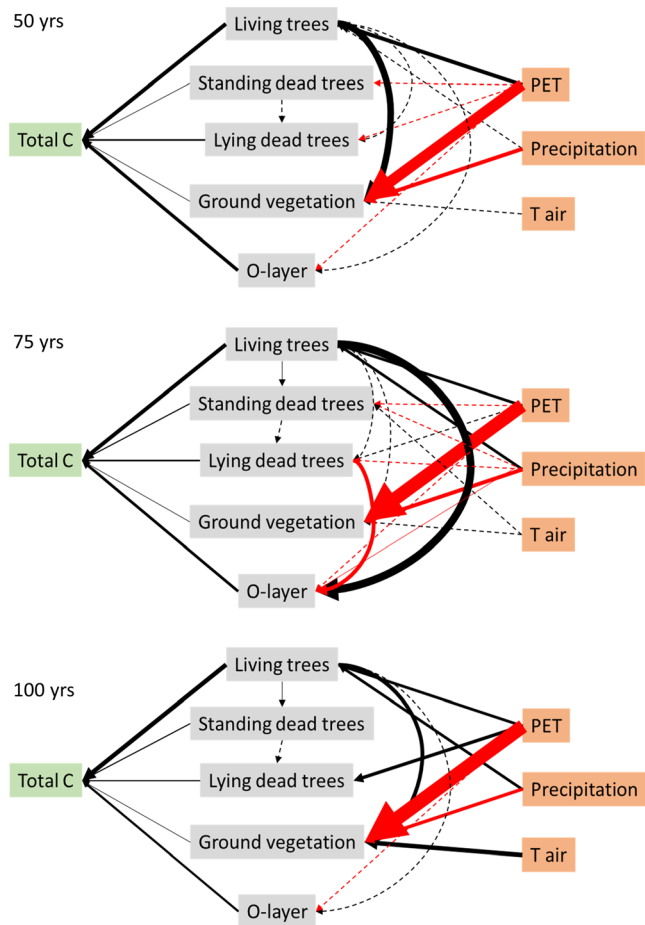


Figure 6. The structural equation models (SEMs) that best fit the data to explain ecosystem carbon stock variability. Arrows indicate direct causal relationships between variables. Black and red arrows represent positive and negative path coefficients, respectively. Arrow widths are proportional to the absolute value of path coefficients. Solid arrows indicate significant ($p \leq 0.05$) and dashed arrows nonsignificant ($p > 0.05$) causal relationships between variables. Overall fit of piecewise SEM was evaluated using Fischer's C statistic (if $p > 0.05$, then no paths are missing and the model is a good fit) and Akaike information criterion (AIC). GPP, gross primary production; O-layer, organic layer; PET, potential evapotranspiration; T air, mean annual air temperature.

Cewise SEM analysis that PET has positive effects on C stocks in living trees and total ecosystem C and a negative effect on C stocks in ground vegetation and O-layer after fire (Figure 6). In the northernmost boreal forests where PET is low, ground vegetation biomass is generally higher than in more southern boreal forests (Helmsaari et al., 2007; Kleja et al., 2008). Low PET also slows down organic matter decomposition (e.g., Berg et al., 1993) and increases C accumulation in the O-layer. In areas where PET is low, forest fire intensity is likely lower (Drever et al., 2008; Littell et al., 2016), which decreases the combustion of the O-layer and thus the loss of C during fire (Czimczik et al., 2005). Our results suggest that productivity (i.e., the development of living tree biomass) plays a major role in the recovery of the C stocks after forest fires in the boreal zone. In contrast, climatic variables were not important factors explaining O-layer C stocks (Figure 6), which may result from favorable climate conditions promoting both litter production and organic matter decomposition. Living trees had a strong increasing effect on the O-layer C stocks in stands that were burned 75 years ago (Figure 6), which is likely due to living tree biomass and litterfall production being high at this age (Chen et al., 2017; Starr et al., 2005). Overall, the significance of living trees in determining total C stocks increased with time since fire, whereas the significance of O-layer decreased with time (Figure 6 and Table 4).

100 years after fire (Figure 5). Living above-ground biomass C stocks (living trees and ground vegetation) were initially only $\leq 10\%$ of the maximum C stock in all the other chronosequences except in chronosequence 1 in Finland (Figure 5).

SEM indicated that total C stocks were strongly dependent on C stocks in the living trees and in the O-layer (Figure 6 and Table 4). It also showed that PET, in turn, was a significant positive driver of C stocks in the living trees. Further, precipitation had a significant positive effect on C stock in living trees. Living trees were a key component of the total ecosystem C stock, often showing positive direct or indirect effects on C stocks in ground vegetation, the O-layer, and standing dead trees. Further, PET negatively affected C stocks in the ground vegetation and O-layer.

4. Discussion

Forest fires play a key role in controlling global C storage (Pellegrini et al., 2018; Walker et al., 2019). Here we show for the first time the decadal-scale recovery of C stocks after wildfires throughout the boreal zone. Previous studies have generally focused on fire-induced direct C emissions (van der Werf et al., 2017), regional representations of C fluxes (e.g., Law et al., 2003; Seedre et al., 2011), or only a specific component of the total C stock such as soil C (Czimczik et al., 2005; Neff et al., 2005) or dead tree C (Brais et al., 2005). Hence, this is the first study that synthesizes information about post-fire C stocks, distribution, and accumulation rates in different ecosystem components in various climatic conditions across the boreal zone, including poorly studied remote regions of the Northern Hemisphere.

Primary production and biomass C stocks in forest ecosystems are broadly correlated with temperature and precipitation (Keith et al., 2009). Our study sites covered a large geographic area where the mean annual temperature varied from -9.5°C to $+5.2^{\circ}\text{C}$ and annual precipitation from 295 to 824 mm. We found that post-fire C stocks in living trees, ground vegetation, and the total ecosystem in the boreal forest can be best explained by PET (Table 3), which integrates temperature, radiation, and the length of the growing season that are important factors that regulate net primary production (Box, 1978; Rosenzweig, 1968). Specifically, we showed through

Table 4

Response Variables ($C \text{ kg m}^{-2}$ in Different Ecosystem Components), Predictors, and Coefficients of Estimates of Structural Equation Models for Chronosequences 50, 75, and 100 Years After Fire

Response variable	Predictor	50-year estimate	75-year estimate	100-year estimate
Total C	Living trees	0.6266 ***	0.6822 ***	0.7388 ***
Total C	O-layer	0.5679 ***	0.4632 ***	0.3942 ***
Total C	Ground vegetation	0.1188 ***	0.0865 ***	0.0863 ***
Total C	Standing dead trees	0.1166 ***	0.1824 ***	0.1877 ***
Total C	Lying dead trees	0.2591 ***	0.2445 *	0.1760 *
Living trees	PET	0.6284 **	0.4711 *	0.4870 *
Living trees	Precipitation	0.3253	0.4934	0.4498
Standing dead trees	PET	-0.4212	-0.4674	
Standing dead trees	Living trees		0.6610	0.2790
Standing dead trees	Precipitation		-0.7881	
Standing dead trees	Temperature		0.4431	
Lying dead trees	Living trees	0.9772	0.4368	
Lying dead trees	Standing dead trees	0.4649		0.2229 *
Lying dead trees	PET	-0.6060	0.5092	0.5960 *
Lying dead trees	Precipitation		-0.4300	
Ground vegetation	Living trees	1.1307 **	0.4850	0.6463 *
Ground vegetation	Temperature	0.5375	0.5742	0.7979 *
Ground vegetation	Precipitation	-0.6837 *		-0.5852 *
Ground vegetation	PET	-1.9122 **	-2.3387 *	-2.3728 **
O-layer	Living trees	0.7720	1.3400	0.6035
O-layer	PET	-0.8371	-0.3455 *	-0.6888
O-layer	Lying dead trees		-0.6962 *	
O-layer	Precipitation		-0.8166 *	

*** $p \leq 0.001$. ** $p \leq 0.01$. * $p \leq 0.05$.

In addition to ecosystem productivity, the severity of fire affects the magnitude of C emissions during combustion (Soja et al., 2004), post-fire vegetation recovery (Ghimire et al., 2012; Kukavskaya et al., 2014; Turner et al., 2019), organic matter decomposition (Boulanger et al., 2011), and subsequent ecosystem C stocks (Ghimire et al., 2012; Lecomte et al., 2006). Fire severity refers to the proportion of consumption of organic material and vegetation mortality that occurs as the direct consequence of a fire (Boby et al., 2010). Comparing the difference in C stocks between recently burned and old sites in our data set suggests that net emissions of C from fires ranged from 0.1 to 11.4 kg m^{-2} , and in most cases, the emissions were $<4 \text{ kg m}^{-2}$ (Figure 2). These values contain a lot of uncertainties and are not directly comparable to directly measured C emissions, but they are, however, the same order of magnitude as previously reported C emissions for forest fires ($0.2\text{--}5.0 \text{ kg m}^{-2}$) in the boreal region (Amiro et al., 2001; Boby et al., 2010; de Groot, Cantin, et al., 2013; French et al., 2011; Kasischke et al., 1995; Kukavskaya et al., 2016; Soja et al., 2004; van Leeuwen et al., 2014; van der Werf et al., 2017).

The observed recovery of C in living trees in our study followed the expected sigmoidal pattern, with slow initial accumulation, rapid accumulation in mid-succession, and finally reduced accumulation in the oldest stands. After low-intensity non-stand-replacing fires such as the Finnish site in our analysis, C stocks in living trees were as high as 2 kg m^{-2} , whereas severe high-intensity stand-replacing fires, which are common in North American boreal forests (de Groot, Cantin, et al., 2013; Kasischke et al., 2005), kill all the trees (Figure 2). The C stock of living tree biomass would have been expected to be about 20% higher if root C would have been measured (Kashian et al., 2013; Repola, 2009). The regeneration of trees after fire seems to be more rapid in more southern and productive climates (Figure 2). In addition to climatic factors, fire severity has an effect on regeneration. Increased soil burn severity improves seedbed conditions and promotes the germination of seeds (Alexander et al., 2018) and deciduous seedling recruitment (Johnstone & Kasischke, 2005). In older stands, living tree biomass had a weak positive effect on dead wood and soil C stocks through litter production (Figure 6).

Mortality of trees and the turnover of organic matter play an important role in the accumulation of C stocks after fire (Bond-Lamberty et al., 2002; Kashian et al., 2013; Seedre et al., 2011; Wirth et al., 2002). Our study

showed that fire killed 30–100% of trees (Figure 2). The C stock in standing dead trees was initially high but declined thereafter, which suggests that fire-killed trees fell and became a part of the downed woody debris pool (Figure 3). Our results are consistent with previous findings that standing dead trees fall during the first 20 years after fire in boreal forests (Figures 2 and 3, Boulanger et al., 2011). Most current Earth system models overestimate C emissions from wildfires because they assume excessive combustion of live trees and do not take into account the standing dead trees that remain as substantial C stocks and decompose over decades after fire (Stenzel et al., 2019). Annual decomposition rate constants for charred wood in boreal forests have been found to vary from 0.013 to 0.052 (Boulanger et al., 2011; Shorohova et al., 2008), which means that 50% of the dead wood C is lost within 13–53 years after fire. In our data set, half of the dead wood C was lost 18–30 years after fire. The link between living trees and standing dead trees strengthened again in later developmental stages of the stands (Figure 6) because tree mortality increases in mature stands (Brais et al., 2005; Seedre et al., 2011).

Stocks of C in the O-layer were low in the first 25 years after fire but increased rapidly thereafter, probably because a pulse of dead wood and the litter of recovering vegetation contributed to soil organic matter formation. In addition, decreased soil microbial biomass (Dooley & Treseder, 2012; Köster et al., 2016) and the formation of recalcitrant (charred) soil organic matter (Aaltonen et al., 2019) may have reduced decomposition rates in post-fire stands (Holden et al., 2015; Köster et al., 2014, 2017; O'Neill et al., 2006) and contributed to C accumulation in the O-layer. There was a large variation in the size and development of C stocks in the O-layer after fire (Figure 3). Spatial variation in soil C stocks is generally high (Harden et al., 2012), and the depth of combustion of the O-layer depends on fire severity (Andrieux et al., 2018), pre-fire organic layer thickness (Grosse et al., 2011), soil bulk density (Grosse et al., 2011), burning conditions (e.g., fire weather), and soil moisture (Grosse et al., 2011; Kasischke et al., 1995). Summertime air temperature best explained the variation in the C pools of the O-layer (Table 3), which reflects the temperature limitation of organic matter decomposition in boreal forests (Hobbie et al., 2000). High summertime temperatures also increase the intensity of forest fires and, consequently, the burning of the O-layer (Lecomte et al., 2006). We found that C stocks in the O-layer were on average 50% lower in recently burned areas compared to old forests (Figure 3). The proportion of O-layer consumed by forest fires can vary greatly depending on fire severity, and fires have been reported to reduce the C stocks of the O-layer by 15–100% in boreal forests (Andrieux et al., 2018; Boby et al., 2010; McRae et al., 2006; Neff et al., 2005; Seedre et al., 2011). Post-fire C accumulation rate in the O-layer in our study varied largely, ranging from 1 to $30 \text{ g m}^{-2} \text{ yr}^{-1}$. The earlier reported values fall between 5 to $40 \text{ g m}^{-2} \text{ yr}^{-1}$ (Czimczik et al., 2005; Harden et al., 2012; Peltoniemi et al., 2004; Wardle et al., 2003).

Total ecosystem C stock (excluding mineral soil C) declined on average by 60% because of fire (Figure 5). For those fires that caused only partial disturbances, the total C stocks declined only by <10%, whereas in the most severe stand-replacing fires, total C stocks declined by $\geq 80\%$ (Figure 5). Accumulation of C was fastest during the first 50 years, and on average, ecosystem C reached 90% of its maximum by 60 years after the fire (Figure 4). Total C stocks accumulated at a rate of $2\text{--}60 \text{ g m}^{-2} \text{ yr}^{-1}$ during the first 100 years. Previously, boreal forests in Canada and Alaska have been reported to accumulate 44 and $50 \text{ g C m}^{-2} \text{ yr}^{-1}$ (including mineral soil C), respectively, during post-fire succession (Alexander & Mack, 2016; Andrieux et al., 2018).

Changes in fire frequency of boreal forests have significant consequences for the global C cycle (Bartowitz et al., 2019; Kasischke et al., 2010; Turner et al., 2019). The recent fire interval has been increased by several hundreds of years because of fire suppression in Fennoscandia and in some parts of North America (Wallenius, 2011). Based on our study, lengthening the fire cycle increases C stocks with the average rates of $13 \text{ g m}^{-2} \text{ yr}^{-1}$ in Eurasian and $29 \text{ g m}^{-2} \text{ yr}^{-1}$ in North American boreal forests. Our results indicated that the C stocks of the O-layer, living trees, and total ecosystem need on average ≥ 100 years for full recovery from fire. Currently, the mean fire return interval is 140–300 years in North American (Kasischke et al., 2010; Ter-Mikaelian et al., 2009) and only 50 years in central Russian boreal forests (de Groot, Cantin, et al., 2013). If climate change in boreal forests causes fires to occur with increasing frequency, as suggested by several studies (de Groot, Cantin, et al., 2013; Kasischke & Turetsky, 2006), these forests may not completely re-accumulate C to pre-fire levels and C sequestration may therefore diminish. However, our results suggest that although climate change likely shortens the fire return interval, increased PET resulting from climate warming (Kellomäki, 2017) speeds up C accumulation and the recovery rate of C stocks in boreal forests.

(Table 3 and Figure 6). The balance between these two processes will ultimately determine the C turnover, and C-climate feedback to the atmosphere, of the global boreal forest.

Data Availability Statement

Data set (<https://doi.org/10.6084/m9.figshare.12758198>) can be downloaded from Figshare data repository (<https://figshare.com>).

Acknowledgments

This research was part of the ARCTICFIRE and BOREALFIRE projects supported by the Academy of Finland (project numbers 286685, 294600, and 307222). We also acknowledge the funding from the Academy of Finland to strengthen university research profiles in Finland for the years 2017–2021 (funding decision 311925) and Reform water-project (funding decision 326818). H. Y. H. Chen acknowledges the funding from the Natural Sciences and Engineering Council of Canada (DG281886-14 and STPGP428641). B. Bond-Lamberty was supported as part of the Energy Exascale Earth System Model (E3SM) project funded by the U.S. Department of Energy, Office of Science, Office of Biological and Environmental Research. A. Prokushkin acknowledges the funding from The Russian Foundation for Basic Research (RFBR #18-05-60203).

References

- Aaltonen, H., Köster, K., Köster, E., Berninger, F., Zhou, X., Karhu, K., et al. (2019). Forest fires in Canadian permafrost region: The combined effects of fire and permafrost dynamics on soil organic matter quality. *Biogeochemistry*, 143(2), 257–274. <https://doi.org/10.1007/s10533-019-00560-x>
- Alexander, H. D., & Mack, M. C. (2016). A canopy shift in interior Alaskan boreal forests: Consequences for above- and belowground carbon and nitrogen pools during post-fire succession. *Ecosystems*, 19(1), 98–114. <https://doi.org/10.1007/s10021-015-9920-7>
- Alexander, H. D., Natali, S. M., Loranty, M. M., Ludwig, S. M., Spektor, V. V., Davydov, S., et al. (2018). Impacts of increased soil burn severity on larch forest regeneration on permafrost soils of far northeastern Siberia. *Forest Ecology and Management*, 417, 144–153. <https://doi.org/10.1016/j.foreco.2018.03.008>
- Amiro, B. D., Barr, A. G., Barr, J. G., Black, T. A., Bracho, R., Brown, M., et al. (2010). Ecosystem carbon dioxide fluxes after disturbance in forests of North America. *Journal of Geophysical Research*, 115, G00K02. <https://doi.org/10.1029/2010JG001390>
- Amiro, B. D., Stocks, B. J., Alexander, M. E., Flannigan, M. D., & Wotton, B. M. (2001). Fire, climate change, carbon and fuel management in the Canadian boreal forest. *International Journal of Wildland Fire*, 10(4), 405–413. <https://doi.org/10.1071/WF01038>
- Andrieux, B., Beguin, J., Bergeron, Y., Grondin, P., & Paré, D. (2018). Drivers of postfire soil organic carbon accumulation in the boreal forest. *Global Change Biology*, 24(10), 4797–4815. <https://doi.org/10.1111/gcb.14365>
- Bartowitz, K. J., Higuera, P. E., Shuman, B. N., McLaughlan, K. K., & Hudiburg, T. W. (2019). Post-fire carbon dynamics in subalpine forests of the Rocky Mountains. *Fire*, 2(4), 58. <https://doi.org/10.3390/fire2040058>
- Berg, B., Berg, M. P., Bottner, P., Box, E., Breymer, A., Calvo de Anta, R., et al. (1993). Litter mass loss rates in pine forests of Europe and eastern United States: Some relationships with climate and litter quality. *Biogeochemistry*, 20(3), 127–159. <https://doi.org/10.1007/BF00000785>
- Boby, L. A., Schuur, E. A. G., Mack, M. C., Verbyla, D., & Johnstone, J. F. (2010). Quantifying fire severity, carbon, and nitrogen emissions in Alaska's boreal forest. *Ecological Applications*, 20(6), 1633–1647. <https://doi.org/10.1890/08-2295.1>
- Bond-Lamberty, B., Peckham, S. D., Ahl, D. E., & Gower, S. T. (2007). Fire as the dominant driver of central Canadian boreal forest carbon balance. *Nature*, 450(7166), 89–92. <https://doi.org/10.1038/nature06272>
- Bond-Lamberty, B., Wang, C., & Gower, S. T. (2002). Coarse woody debris and its annual carbon flux for a boreal black spruce fire chronosequence. *Journal of Geophysical Research*, 108(D3), 8220. <https://doi.org/10.1029/2001JD000839>
- Bormann, F. H., & Likens, G. E. (1979). *Pattern and process in a forested ecosystem: Disturbance, development and the steady state based on the Hubbard Brook ecosystem study*. New York, NY: Springer-Verlag. <https://doi.org/10.1007/978-1-4612-6232-9>
- Boulanger, Y., Sirois, L., & Hébert, C. (2011). Fire severity as a determinant factor of the decomposition rate of fire-killed black spruce in the northern boreal forest. *Canadian Journal of Forest Research*, 41(2), 370–379. <https://doi.org/10.1139/X10-218>
- Box, E. (1978). Geographical dimensions of terrestrial net and gross primary productivity. *Radiation and Environmental Biophysics*, 15(4), 305–322. <https://doi.org/10.1007/BF01323458>
- Brais, S., Sadi, F., Bergeron, Y., & Grenier, Y. (2005). Coarse woody debris dynamics in a post-fire jack pine chronosequence and its relation with site productivity. *Forest Ecology and Management*, 220(1–3), 216–226. <https://doi.org/10.1016/j.foreco.2005.08.013>
- Chen, H. Y. H., Brant, A. N., Seedre, M., Brassard, B. W., & Taylor, A. R. (2017). The contribution of litterfall to net primary production during secondary succession in the boreal forest. *Ecosystems*, 20, 830–844.
- Czimczik, C. I., Schmidt, M. W. I., & Schulze, E.-D. (2005). Effects of increasing fire frequency on black carbon and organic matter in Podzols of Siberian Scots pine forests. *European Journal of Soil Science*, 56(3), 417–428. <https://doi.org/10.1111/j.1365-2389.2004.00665.x>
- de Groot, W. J., Cantin, A. S., Flannigan, M. D., Soja, A. J., Gowman, L. M., & Newberry, A. (2013). A comparison of Canadian and Russian boreal forest fire regimes. *Forest Ecology and Management*, 294, 23–34. <https://doi.org/10.1016/j.foreco.2012.07.033>
- de Groot, W. J., Flannigan, M. D., & Cantin, A. S. (2013). Climate change impacts on future boreal fire regimes. *Forest Ecology and Management*, 294, 35–44. <https://doi.org/10.1016/j.foreco.2012.09.027>
- DeLuca, T. H., & Boisvenue, C. (2012). Boreal forest soil carbon: Distribution, function and modelling. *Forestry*, 85(2), 161–184. <https://doi.org/10.1093/forestry/cps003>
- DeLuca, T. H., Nilsson, M. C., & Zackrisson, O. (2002). Nitrogen mineralization and phenol accumulation along a fire chronosequence in northern Sweden. *Oecologia*, 133(2), 206–214. <https://doi.org/10.1007/s00442-002-1025-2>
- Dooley, S. R., & Treseder, K. K. (2012). The effect of fire on microbial biomass: A meta-analysis of field studies. *Biogeochemistry*, 109(1–3), 49–61. <https://doi.org/10.1007/s10533-011-9633-8>
- Drever, C. R., Drever, M. C., Messier, C., Bergeron, Y., & Flannigan, M. (2008). Fire and the relative roles of weather, climate and landscape characteristics in the Great Lakes-St. Lawrence forest of Canada. *Journal of Vegetation Science*, 19(1), 57–66. <https://doi.org/10.3170/2007-8-18313>
- Fan, Y., Chen, J., Shirkey, G., John, R., Wu, S. R., Park, H., & Shao, C. (2016). Applications of structural equation modeling (SEM) in ecological studies: An updated review. *Ecological Processes*, 5(1), 19. <https://doi.org/10.1186/s13717-016-0063-3>
- Flannigan, M., Stocks, B., Turetsky, M., & Wotton, M. (2009). Impacts of climate change on fire activity and fire management in the circumboreal forest. *Global Change Biology*, 15(3), 549–560. <https://doi.org/10.1111/j.1365-2486.2008.01660.x>
- French, N. H. F., de Groot, W. J., Jenkins, L. K., Rogers, B. M., Alvarado, E., Amiro, B., et al. (2011). Model comparisons for estimating carbon emissions from North American wildland fire. *Journal of Geophysical Research*, 116, G00K05. <https://doi.org/10.1029/2010JG001469>
- Gao, B., Taylor, A. R., Searle, E. B., Kumar, P., Ma, Z., Hume, A., & Chen, H. Y. H. (2018). Carbon storage declines in old boreal forests irrespective of succession pathway. *Ecosystems*, 21(6), 1168–1182. <https://doi.org/10.1007/s10021-017-0210-4>

- Ghimire, B., Williams, C. A., Collatz, G. J., & Vanderhoof, M. (2012). Fire-induced carbon emissions and regrowth uptake in western U.S. forests: Documenting variation across forest types, fire severity, and climate regions. *Journal of Geophysical Research*, 117, G03036. <https://doi.org/10.1029/2011JG001935>
- Grosse, G., Harden, J., Turetsky, M., McGuire, A. D., Camill, P., Tarnocai, C., et al. (2011). Vulnerability of high-latitude soil organic carbon in North America to disturbance. *Journal of Geophysical Research*, 116, G00K06. <https://doi.org/10.1029/2010JG001507>
- Harden, J. W., Manies, K. L., O'Donnell, J., Johnson, K., Frolking, S., & Fan, Z. (2012). Spatiotemporal analysis of black spruce forest soils and implications for the fate of C. *Journal of Geophysical Research*, 117, G01012. <https://doi.org/10.1029/2011JG001826>
- Harden, J. W., Mark, R. K., Sundquist, E. T., & Stallard, R. F. (1992). Dynamics of soil carbon during deglaciation of the Laurentide ice sheet. *Science*, 258(5090), 1921–1924. <https://doi.org/10.1126/science.258.5090.1921>
- Helmisaari, H.-S., Derome, J., Nöjd, P., & Kukkola, M. (2007). Fine root biomass in relation to site and stand characteristics in Norway spruce and Scots pine stands. *Tree Physiology*, 27(10), 1493–1504. <https://doi.org/10.1093/treephys/27.10.1493>
- Hobbie, S. E., Schimel, J. P., Trumbore, S. E., & Randerson, J. R. (2000). Controls over carbon storage and turnover in high-latitude soils. *Global Change Biology*, 6(S1), 196–210. <https://doi.org/10.1046/j.1365-2486.2000.06021.x>
- Holden, S. R., Berhe, A. A., & Treseder, K. K. (2015). Decreases in soil moisture and organic matter quality suppress microbial decomposition following a boreal forest fire. *Soil Biology and Biochemistry*, 87, 1–9. <https://doi.org/10.1016/j.soilbio.2015.04.005>
- Johnstone, J. F., Allen, C. D., Franklin, J. F., Frelich, L. E., Harvey, B. J., Higuera, P. E., et al. (2016). Changing disturbance regimes, ecological memory, and forest resilience. *Frontiers in Ecology and the Environment*, 14(7), 369–378. <https://doi.org/10.1002/fee.1311>
- Johnstone, J. F., & Kasischke, E. S. (2005). Stand-level effects of soil burn severity on postfire regeneration in a recently burned black spruce forest. *Canadian Journal of Forest Research*, 35(9), 2151–2163. <https://doi.org/10.1139/x05-087>
- Kashian, D. M., Romme, W. H., Tinker, D. B., Turner, M. G., & Ryan, M. G. (2013). Postfire changes in forest carbon storage over a 300-year chronosequence of *Pinus contorta*-dominated forests. *Ecological Monographs*, 83(1), 49–66. <https://doi.org/10.1890/11-1454.1>
- Kasischke, E. S., Christensen, N. L. Jr., & Stocks, B. J. (1995). Fire, global warming, and the carbon balance of boreal forests. *Ecological Applications*, 5(2), 437–451. <https://doi.org/10.2307/1942034>
- Kasischke, E. S., Hyer, E. J., Novelli, P. C., Bruhwiler, L. P., French, N. H. F., Sukhinin, A. I., et al. (2005). Influences of boreal fire emissions on Northern Hemisphere atmospheric carbon and carbon monoxide. *Global Biogeochemical Cycles*, 19, GB1012. <https://doi.org/10.1029/2004GB002300>
- Kasischke, E. S., & Turetsky, M. R. (2006). Recent changes in the fire regime across the North American boreal region spatial and temporal patterns of burning across Canada and Alaska. *Geophysical Research Letters*, 33, L09703. <https://doi.org/10.1029/2006GL025677>
- Kasischke, E. S., Verbyla, D. L., Rupp, T. S., McGuire, A. D., Murphy, K. A., Jandt, R., et al. (2010). Alaska's changing fire regime—implications for the vulnerability of its boreal forests. *Canadian Journal of Forest Research*, 40(7), 1313–1324. <https://doi.org/10.1139/X10-098>
- Keith, H., Mackey, B. G., & Lindenmayer, D. B. (2009). Re-evaluation of forest biomass carbon stocks and lessons from the world's most carbon-dense forests. *PNAS*, 106(28), 11,635–11,640. <https://doi.org/10.1073/pnas.0901970106>
- Kellomäki, S. (2017). Climate change in the local context, with changes in growing conditions. In *Managing boreal forests in the context of climate change. Impacts, adaptation and climate change mitigation*. Boca Raton, Florida, USA: CRC Press. <https://doi.org/10.1201/9781315166063>
- Kleja, D. B., Svensson, M., Majdi, H., Jansson, P. E., Langvall, O., Bergkvist, B., et al. (2008). Pools and fluxes of carbon in three Norway spruce ecosystems along a climatic gradient in Sweden. *Biogeochemistry*, 89(1), 7–25. <https://doi.org/10.1007/s10533-007-9136-9>
- Köster, E., Köster, K., Berninger, F., Aaltonen, H., Zhou, X., & Pumpanen, J. (2017). Carbon dioxide, methane and nitrous oxide fluxes from a fire chronosequence in subarctic boreal forests of Canada. *Science of the Total Environment*, 601–602, 895–905. <https://doi.org/10.1016/j.scitotenv.2017.05.246>
- Köster, E., Köster, K., Berninger, F., Prokushkin, A., Aaltonen, H., Zhou, X., & Pumpanen, J. (2018). Changes in fluxes of carbon dioxide and methane caused by fire in Siberian boreal forest with continuous permafrost. *Journal of Environmental Management*, 228, 405–415. <https://doi.org/10.1016/j.jenvman.2018.09.051>
- Köster, K., Berninger, F., Lindén, A., Köster, E., & Pumpanen, J. (2014). Recovery in fungal biomass is related to decrease in soil organic matter turnover time in a boreal fire chronosequence. *Geoderma*, 235–236, 74–82. <https://doi.org/10.1016/j.geoderma.2014.07.001>
- Köster, K., Köster, E., Orumaa, A., Parro, K., Jögiste, K., Berninger, F., et al. (2016). How time since forest fire affects stand structure, soil physical-chemical properties and soil CO₂ efflux in Hemiboreal Scots pine forest fire chronosequence? *Forests*, 7(12), 201. <https://doi.org/10.3390/f7090201>
- Kukavskaya, E. A., Buryak, L. V., Shvetsov, E. G., Conard, S. G., & Kalenskaya, O. P. (2016). The impact of increasing fire frequency on forest transformations in southern Siberia. *Forest Ecology and Management*, 382, 225–235. <https://doi.org/10.1016/j.foreco.2016.10.015>
- Kukavskaya, E. A., Ivanova, G. A., Conard, S. G., McRae, D. J., & Ivanov, V. A. (2014). Biomass dynamics of central Siberian Scots pine forests following surface fires of varying severity. *International Journal of Wildland Fire*, 23(6), 872–886. <https://doi.org/10.1071/WF13043>
- Kurz, W. A., Shaw, C. H., Boisvenue, C., Stinson, G., Metsaranta, J., Leckie, D., & Neilson, E. T. (2013). Carbon in Canada's boreal forest—A synthesis. *Environmental Reviews*, 21(4), 260–292. <https://doi.org/10.1139/er-2013-0041>
- Lambert, M.-C., Ung, C.-H., & Raulier, F. (2005). Canadian national tree aboveground biomass equations. *Canadian Journal of Forest Research*, 35(8), 1996–2018. <https://doi.org/10.1139/x05-112>
- Larjavaara, M., Berninger, F., Palviainen, M., Prokushkin, A., & Wallenius, T. (2017). Post-fire carbon and nitrogen accumulation and succession in Central Siberia. *Scientific Reports*, 7(1), 12776. <https://doi.org/10.1038/s41598-017-13039-2>
- Law, B. E., Sun, O. J., Campbell, J., van Tuyl, S., & Thornton, P. E. (2003). Changes in carbon storage and fluxes in chronosequence of ponderosa pine. *Global Change Biology*, 9(4), 510–524. <https://doi.org/10.1046/j.1365-2486.2003.00624.x>
- Le Quéré, C., Andrew, R. M., Friedlingstein, P., Sitch, S., Hauck, J., Pongratz, J., et al. (2018). Global carbon budget 2018. *Earth System Science Data*, 10(4), 2141–2194. <https://doi.org/10.5194/essd-10-2141-2018>
- Lecomte, N., Simard, M., Fenton, N., & Bergeron, Y. (2006). Fire severity and long-term ecosystem biomass dynamics in coniferous boreal forests of Eastern Canada. *Ecosystems*, 9(8), 1215–1230. <https://doi.org/10.1007/s10021-004-0168-x>
- Lefcheck, J. S. (2016). PIECEWISESEM: Piecewise structural equation modelling in R for ecology, evolution, and systematics. *Methods in Ecology and Evolution*, 7(5), 573–579. <https://doi.org/10.1111/2041-210X.12512>
- Lehtonen, I., Venäläinen, A., Kämäräinen, M., Peltola, H., & Gregow, H. (2016). Risk of large-scale fires in boreal forests of Finland under changing climate. *Natural Hazards and Earth System Sciences*, 16(1), 239–253. <https://doi.org/10.5194/nhess-16-239-2016>

- Li, F., Lawrence, D. M., & Bond-Lamberty, B. (2017). Impact of fire on global land surface air temperature and energy budget for the 20th century due to changes within ecosystems. *Environmental Research Letters*, 12(4), 044014. <https://doi.org/10.1088/1748-9326/aa6685>
- Littell, J. S., Peterson, D. L., Riley, K. L., Liu, Y., & Luce, C. H. (2016). A review of the relationships between drought and forest fire in the United States. *Global Change Biology*, 22(7), 2353–2369. <https://doi.org/10.1111/gcb.13275>
- Luyssaert, S., Schulze, E. D., Börner, A., Knöhl, A., Hessenmöller, D., Law, B. E., et al. (2008). Old-growth forests as global carbon sinks. *Nature*, 455(7210), 213–215. <https://doi.org/10.1038/nature07276>
- Marklund, L. G. (1988). *Biomassafunktioner för tall, gran och björk i Sverige* (p. 73). Umeå, Sweden: Sveriges Lantbruksuniversitet.
- McRae, D. J., Conard, S. G., Ivanova, G. A., Sukhinin, A. I., Baker, S. P., Samsonov, Y. N., et al. (2006). Variability of fire behavior, fire effects, and emissions in Scotch pine forests of central Siberia. *Mitigation and Adaptation Strategies for Global Change*, 11(1), 45–74. <https://doi.org/10.1007/s11027-006-1008-4>
- Nave, L. E., Vance, E. D., Swanston, C. W., & Curtis, P. S. (2011). Fire effects on temperate forest soil C and N storage. *Ecological Applications*, 21(4), 1189–1201. <https://doi.org/10.1890/10-0660.1>
- Neff, J. C., Harden, J. W., & Gleixner, G. (2005). Fire effects on soil organic matter content, composition, and nutrients in boreal interior Alaska. *Canadian Journal of Forest Research*, 35(9), 2178–2187. <https://doi.org/10.1139/X05-154>
- New, M., Hulme, M., & Jones, P. (2000). Representing twentieth-century space-time climate variability. Part II: Development of 1901–96 monthly grids of terrestrial surface climate. *Journal of Climate*, 13(13), 2217–2238. [https://doi.org/10.1175/1520-0442\(2000\)013<2217:RTCSTC>2.0.CO;2](https://doi.org/10.1175/1520-0442(2000)013<2217:RTCSTC>2.0.CO;2)
- O'Neill, K. P., Richter, D. D., & Kasischke, E. S. (2006). Succession-driven changes in soil respiration following fire in black spruce stands of interior Alaska. *Biogeochemistry*, 80(1), 1–20. <https://doi.org/10.1007/s10533-005-5964-7>
- Palmer, W. C. (1965). Meteorological Drought. Research Paper No. 45, Weather Bureau, US Department of Commerce, Washington, DC.
- Palviaainen, M., Pumpanen, J., Berninger, F., Ritala, K., Duan, B., Heinonsalo, J., et al. (2017). Nitrogen balance along a northern boreal forest fire chronosequence. *PLoS ONE*, 12(3), e0174720. <https://doi.org/10.1371/journal.pone.0174720>
- Pan, Y., Birdsey, R. A., Fang, J., Houghton, R., Kauppi, P. E., Kurz, W. A., et al. (2011). A large and persistent carbon sink in the world's forests. *Science*, 333(6045), 988–993. <https://doi.org/10.1126/science.1201609>
- Paré, D., Bernier, P., Lafleur, B., Titus, B. D., Thiffault, E., Maynard, D. G., & Guo, X. (2013). Estimating stand-scale biomass, nutrient contents, and associated uncertainties for tree species of Canadian forests. *Canadian Journal of Forest Research*, 43(7), 599–608. <https://doi.org/10.1139/cjfr-2012-0454>
- Pellegrini, A. F. A., Ahlström, A., Hobbie, S. E., Reich, P. B., Nieradzik, L. P., Staver, A. C., et al. (2018). Fire frequency drives decadal changes in soil carbon and nitrogen and ecosystem productivity. *Nature*, 553(7687), 194–198. <https://doi.org/10.1038/nature24668>
- Peltoniemi, M., Mäkipää, R., Liski, J., & Tamminen, P. (2004). Changes in soil carbon with stand age—An evaluation of a modelling method with empirical data. *Global Change Biology*, 10(12), 2078–2091. <https://doi.org/10.1111/j.1365-2486.2004.00881.x>
- Ponomarev, E. I., Kharuk, V. I., & Ranson, K. J. (2016). Wildfires dynamics in Siberian larch forests. *Forests*, 7(12), 125. <https://doi.org/10.3390/f7060125>
- Randerson, J. T., Liu, H., Flanner, M. G., Chambers, S. D., Jin, Y., Hess, P. G., et al. (2006). The impact of boreal forest fire on climate warming. *Science*, 314(5802), 1130–1132. <https://doi.org/10.1126/science.1132075>
- Repola, J. (2008). Biomass equations for birch in Finland. *Silva Fennica*, 42, 605–624.
- Repola, J. (2009). Biomass equations for Scots pine and Norway spruce in Finland. *Silva Fennica*, 43, 625–647.
- Rogers, B. M., Soja, A. J., Goulden, M. L., & Randerson, J. T. (2015). Influence of tree species on continental differences in boreal fires and climate feedbacks. *Nature Geoscience*, 8(3), 228–234. <https://doi.org/10.1126/science.113207510.1038/NGEO2352>
- Rosenzweig, M. L. (1968). Net primary productivity of terrestrial communities: Prediction from climatological data. *The American Naturalist*, 102(923), 67–74. <https://doi.org/10.1086/282523>
- Seedre, M., Shrestha, B. M., Chen, H. Y. H., Colombo, S., & Jögiste, K. (2011). Carbon dynamics of North American boreal forest after stand replacing wildfire and clearcut logging. *Journal of Forest Research*, 16(3), 168–183. <https://doi.org/10.1007/s10310-011-0264-7>
- Seedre, M., Taylor, A. R., Brassard, B. W., Chen, H. Y. H., & Jögiste, K. (2014). Recovery of ecosystem carbon stocks in young boreal forests: A comparison of harvesting and wildfire disturbance. *Ecosystems*, 17(5), 851–863. <https://doi.org/10.1007/s10021-014-9763-7>
- Shorohova, E., Kapitsa, E., & Vanha-Majamaa, I. (2008). Decomposition of stumps in a chronosequence after clear-felling vs. clear-felling with prescribed burning in a southern boreal forest in Finland. *Forest Ecology and Management*, 255(10), 3606–3612. <https://doi.org/10.1016/j.foreco.2008.02.042>
- Simard, M., Lecomte, N., Bergeron, Y., Bernier, P. Y., & Paré, D. (2007). Forest productivity decline caused by successional paludification of boreal soils. *Ecological Applications*, 17(6), 1619–1637. <https://doi.org/10.1890/06-1795.1>
- Soja, A. J., Cofer, W. R., Shugart, H. H., Sukhinin, A. I., Stackhouse, P. W. Jr., McRae, D. J., & Conard, S. G. (2004). Estimating fire emissions and disparities in boreal Siberia (1998–2002). *Journal of Geophysical Research*, 109, D14S06. <https://doi.org/10.1029/2004JD004570>
- Starr, M., Saarsalmi, A., Hokkanen, T., Merilä, P., & Helmsaari, H.-S. (2005). Models of litterfall production for Scots pine (*Pinus sylvestris* L.) in Finland using stand, site and climate factors. *Forest Ecology and Management*, 205(1–3), 215–225. <https://doi.org/10.1016/j.foreco.2004.10.047>
- Stenzel, J. E., Bartowitz, K. J., Hartman, M. D., Lutz, J. A., Kolden, C. A., Smith, A. M. S., et al. (2019). Fixing a snag in carbon emissions estimates from wildfires. *Global Change Biology*, 25(11), 3985–3994. <https://doi.org/10.1111/gcb.14716>
- Taylor, A. R., Seedre, M., Brassard, B. W., & Chen, H. Y. H. (2014). Decline in net ecosystem productivity following canopy transition to late-succession forests. *Ecosystems*, 17(5), 778–791. <https://doi.org/10.1007/s10021-014-9759-3>
- Ter-Mikaelian, M. T., Colombo, S. J., & Chen, J. (2009). Estimating natural forest fire return interval in northeastern Ontario, Canada. *Forest Ecology and Management*, 258(9), 2037–2045. <https://doi.org/10.1016/j.foreco.2009.07.056>
- Turner, M. G., Braziunas, K. H., Hansen, W. D., & Harvey, B. J. (2019). Short-interval severe fire erodes the resilience of subalpine lodgepole pine forests. *PNAS*, 116(23), 11,319–11,328. www.pnas.org/cgi/doi/10.1073/pnas.1902841116
- van Bellen, S., Garneau, M., & Bergeron, Y. (2010). Impact of climate change on forest fire severity and consequences for carbon stocks in boreal forest stands of Quebec, Canada: A synthesis. *Fire Ecology*, 6(3), 16–44. <https://doi.org/10.4996/fireecology.0603016>
- van der Werf, G. R., Randerson, J. T., Giglio, L., van Leeuwen, T. T., Chen, Y., Rogers, B. M., et al. (2017). Global fire emissions estimates during 1997–2016. *Earth System Science Data*, 9(2), 697–720. <https://doi.org/10.5194/essd-9-697-2017>
- van Leeuwen, T. T., van der Werf, G. R., Hoffmann, A. A., Detmers, R. G., Rücker, G., French, N., et al. (2014). Biomass burning fuel consumption rates: A field measurement database. *Biogeosciences*, 11(24), 7305–7329. <https://doi.org/10.5194/bg-11-7305-2014>
- Walker, L. R., Wardle, D. A., Bardgett, R. D., & Clarkson, B. D. (2010). The use of chronosequences in studies of ecological succession and soil development. *Journal of Ecology*, 98(4), 725–736. <https://doi.org/10.1111/j.1365-2745.2010.01664.x>

- Walker, X. J., Baltzer, J. L., Cumming, S. G., Day, N. J., Ebert, C., Goetz, S., et al. (2019). Increasing wildfires threaten historic carbon sink of boreal forest soils. *Nature*, 572(7770), 520–523. <https://doi.org/10.1038/s41586-019-1474-y>
- Wallenius, T. (2011). Major decline in fires in coniferous forests—Reconstructing the phenomenon and seeking for the cause. *Silva Fennica*, 45(1), 139–155.
- Wang, C., Bond-Lamberty, B., & Gower, S. T. (2003). Carbon distribution of a well- and poorly drained black spruce fire chronosequence. *Global Change Biology*, 9(7), 1066–1079. <https://doi.org/10.1046/j.1365-2486.2003.00645.x>
- Ward, C., Pothier, D., & Paré, D. (2014). Do boreal forests need fire disturbance to maintain productivity? *Ecosystems*, 17(6), 1053–1067. <https://doi.org/10.1007/s10021-014-9782-4>
- Wardle, D. A., Hörnberg, G., Zackrisson, O., Kalela-Brundin, M., & Coomes, D. A. (2003). Long-term effects of wildfire on ecosystem properties across an island area gradient. *Science*, 300(5621), 972–975. <https://doi.org/10.1126/science.1082709>
- Wardle, D. A., Walker, L. R., & Bardgett, R. D. (2004). Ecosystem properties and forest decline in contrasting long-term chronosequences. *Science*, 305(5683), 509–513. <https://doi.org/10.1126/science.1098778>
- Williams, C. A., Gua, H., MacLean, R., Masek, J. G., & Collatz, G. J. (2016). Disturbance and the carbon balance of US forests: A quantitative review of impacts from harvests, fires, insects, and droughts. *Global and Planetary Change*, 143, 66–80. <https://doi.org/10.1016/j.gloplacha.2016.06.002>
- Wirth, C., Schulze, E.-D., Lühker, B., Grigoriev, S., Siry, M., Hardes, G., et al. (2002). Fire and site type effects on the long-term carbon and nitrogen balance in pristine Siberian Scots pine forests. *Plant and Soil*, 242(1), 41–63. <https://doi.org/10.1023/A:1020813505203>
- Zhou, G., Liu, S., Li, Z., Zhang, D., Tang, X., Zhou, C., & Mo, J. (2006). Old-growth forests can accumulate carbon in soils. *Science*, 314(5804), 1417. <https://doi.org/10.1126/science.1130168>